symmetry

MDPI

Article

Docking of Cisplatin on Fullerene Derivatives and Some Cube Rhombellane Functionalized Homeomorphs

Beata Szefler * and Przemysław Czeleń

Department of Physical Chemistry, Faculty of Pharmacy, Collegium Medicum, Nicolaus Copernicus University, Kurpińskiego 5, 85-096, Bydgoszcz, Poland

* Correspondence: beatas@cm.umk.pl

Received: 12 June 2019; Accepted: 27 June 2019; Published: 3 July 2019

Abstract: Cisplatin (cisPt) is one of the strongest anticancer agents with proven clinical activity against a wide range of solid tumors. Its mode of action has been linked to its ability to crosslink with the canonical purine bases, primarily with guanine. Theoretical studies performed at the molecular level suggest that such nonspecific interactions can also take place with many competitive compounds, such as vitamins of the B group, containing aromatic rings with lone-pair orbitals. This might be an indicator of reduction of the anticancer therapeutic effects of the Cisplatin drug in the presence of vitamins of the B group inside the cell nucleus. That is why it seems to be important to connect CisPt with nanostructures and in this way prevent the drug from combining with the B vitamins. As a proposal for a new nanodrug, an attempt was made to implement Cispaltin (CisPt) ligand on functionalized C_{60} fullerenes and on a cube rhombellane homeomorphic surface. The symmetry of the analyzed nanostructures is an important factor determining the mutual affinity of the tested ligand and nanocarriers. The behavior of Cisplatin with respect to rhombellane homeomorphs and functionalized fullerenes C_{60}, in terms of their (interacting) energy, geometry and topology was studied and a detailed analysis of structural properties after docking showed many interesting features.

Keywords: cube rhombellane homeomorph; functionalized fullerene C_{60}; Cisplatin (CisPt), nanostructure; molecular docking; affinity

1. Introduction

Cisplatinum (cisPt) (Figure 1) is one of the strongest anticancer agents with proven clinical activity against a wide range of solid tumors [1–5]. As a chemotherapeutic drug it has been used for treatment of numerous human cancers including lung, bladder, testicular, head, and neck cancers [1] and ovarian carcinomas [4]. It is effective against various types of cancers, including carcinomas, lymphomas, germ cell tumors and sarcomas [2]. Its mode of action has been linked to its ability to crosslink with the canonical purine bases, primarily with guanine, and to a lesser extent with adenine, found within double helical DNA. This in turn seriously interferes with DNA repair mechanisms, causing DNA damage and subsequently inducing apoptosis [6] in cancer cells.

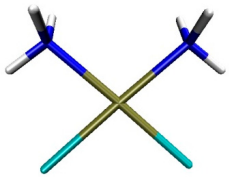

Figure 1. Cisplatinum (cisPt; $[Pt(NH_3)_2Cl_2]$) [5].

However, theoretical studies performed at the molecular level suggest that such nonspecific interactions can also take place with many competitive compounds, such as vitamins containing aromatic rings with lone-pair orbitals [7]. It is argued that such direct analogy to interactions with canonical purines can impair the therapeutic effect of Cisplatin. This might be an indicator of reduction of the anticancer therapeutic effects of the Cisplatin drug in the presence of vitamins of the B group inside the cell nucleus [7].

That is why it seems to be important to connect CisPt with nanostructures and in this way make it prevent the drug from combining with the B vitamins. After passing through the cellular barrier, a rupture of the complex would occur and the free cisPt could interact with bases in the interior of the cell (Figure 2).

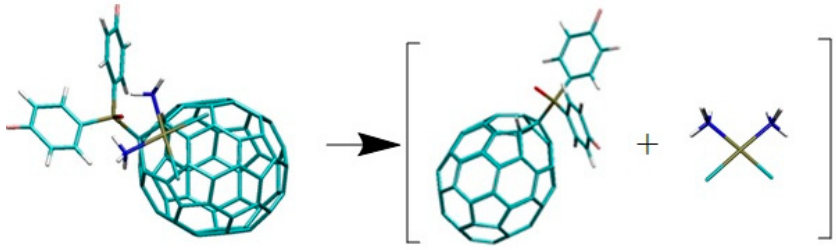

Figure 2. Rupture of the complex after passing through the cellular barrier.

Rhombellans are new structures defined by Diudea [8–13] with rings in the form of rhombs or squares, which could be an alternative to classical carrier nanostructures. This new class of compounds, having drug-like properties, and creating bio-nano devices, can be suitable for medical chemistry.

Rhombellanes have certain specific features: (i) all strong rings are squares/rhombs; (ii) vertex classes consist of only non-connected vertices; (iii) the Omega polynomial has a single term: 1X^|E|; (iv) a line graph of the parent graph has a Hamiltonian circuit; and (v) they contain at least one $K_{2.3}$ complete bipartite subgraph or the smallest rhombellane Rbl.5.

Rhombellanes may be synthesized as real molecules, which represent a new class of hypothetical structures. Quantum calculations (at the B3LYP/6-31G (d, p) level of theory) [14,15] support the hypothesis that these substructures (at every level of complexity) are energetically feasible in the hope of a real synthesis [16–20].

There are many types of these structures, among which only those have been used which have functional groups that allow attachment of CisPt (Figure 3).

ful_308a4 ful_308b4

Figure 3. *Cont.*

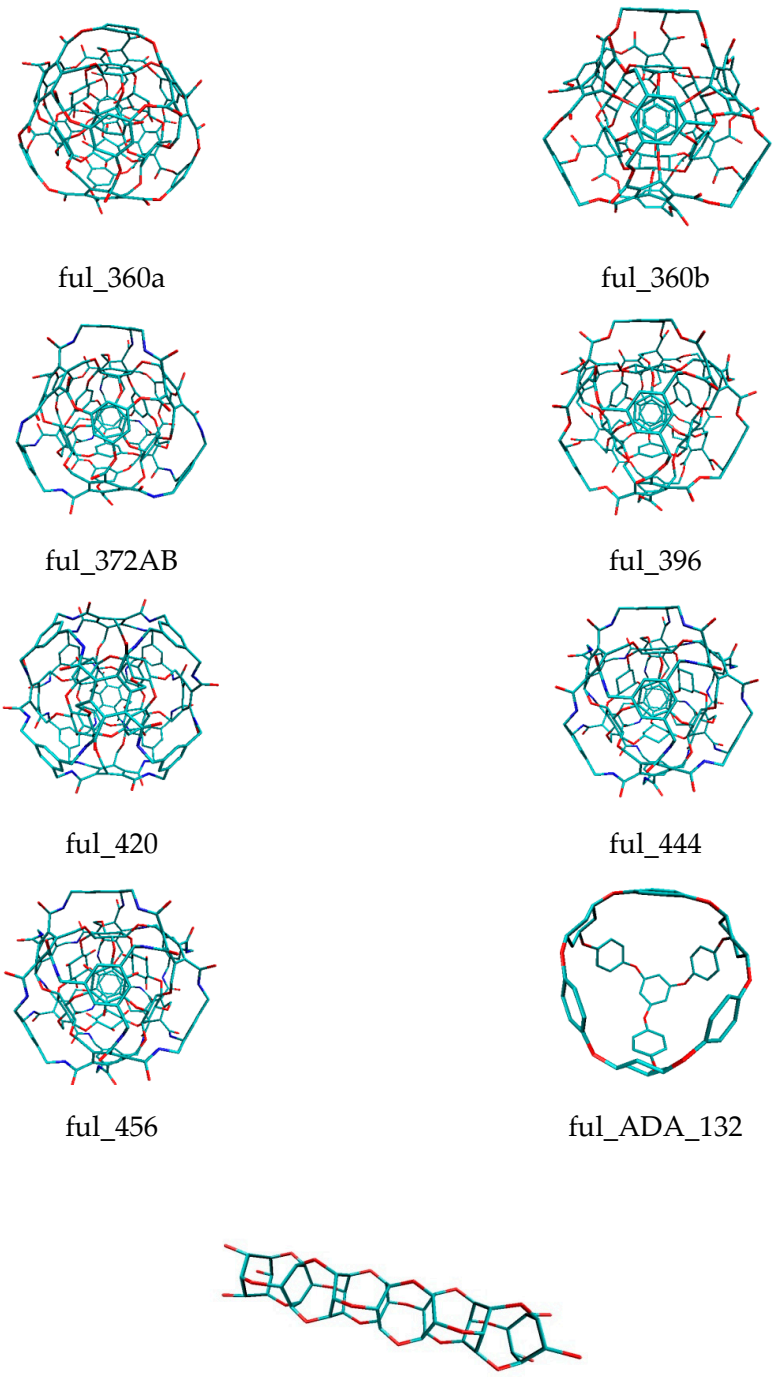

Figure 3. Graphic representation of the cube rhombellanes.

Despite the initially expected chemical inactivity of C_{60} and its derivatives, it was found that fullerenes can be functionalized [21]. Due to the mode of functionalization, there were distinguished exo- and endohedral forms of fullerenes and heterofullerenes. The essence of exohedral chemistry is the chemical reactions of attachment "outside" of fullerene molecules, in which the structure of the carbon cage remains unchanged. Unlike other organic, aliphatic and aromatic compounds, fullerenes do not contain hydrogen atoms or other functional groups,

so they cannot undergo substitution reactions (except for Heterofullerens). Substitution reactions occur only with "functionalized" fullerenes, i.e. when they have been attached to specific groups of atoms. C_{60} and its homologues have interesting and often unique properties, and after functionalization the C_{60} molecule can bind any functional group (Figure 4) [21]. At the same time, it is indifferent, non-toxic and so small that it easily comes into contact with cells, proteins and viruses. In the docking procedure with Cisplatin several exohedral forms of C_{60} fullerenes were used, such as 1-(Diethoxyphosphorylmethyl)-7-(2,2,2-trifluoroethoxy)(C_{60}-Ih)[5,6]fullerene;9-(diethoxyphosphorylmethyl)-1H-(C_{60}-Ih)[5,6]fullerene;

Methyl 9-(2-trimethylsilylethyl)(C_{60}-Ih)[5,6]fullerene-1-carboxylate and others (Figure 4).

CID_ 11332103.
$C_{67}H_{14}F_3O_4P$
1-(Diethoxyphosphoryl methyl) -7-(2,2,2-trifluoroethoxy)(C_{60}-Ih)[5,6]fullerene

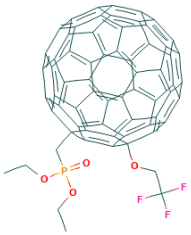

CID_11468612
$C_{65}H_{13}O_3P$
9-(diethoxyphosphoryl methyl)-1H- (C_{60}-Ih)[5,6]fullerene

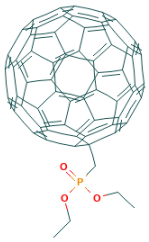

CID_16146387
$C_{67}H_{16}O_2Si$
Methyl 9-(2-trimethylsilylethyl) (C_{60}-Ih)[5,6]fullerene-1-carboxylate

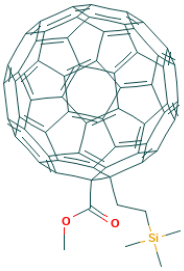

CID_16150529
$C_{70}H_{20}N_2O_2$
1-N,1-N,9-N,9-N-Tetraethyl(C_{60}-Ih)[5,6]fullerene-1,9-dicarboxamide

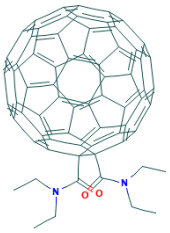

CID_16156307
$C_{72}H_9F_2OP$
9-Bis(4-fluorophenyl)phosphoryl-1H-(C_{60}-Ih)[5,6]fullerene

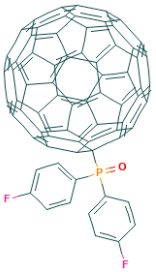

CID_71619159
$C_{68}H_{10}O_2$
9-(2,4-Dimethoxyphenyl)-1H-(C_{60}-Ih)[5,6]fullerene

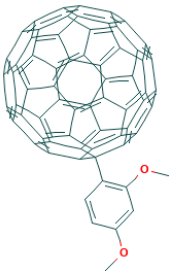

CID_101218232
$C_{63}H_4ClF_3O$
1-(Chloromethyl)-7-(2,2,2-trifluoroethoxy)(C_{60}-Ih)[5,6]fullerene

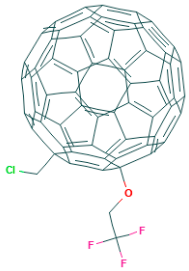

CID_101218236
$C_{69}H_9Cl_3O$
1-(4-Methoxyphenyl)-7-(1,1,2-trichloroethyl)(C_{60}-Ih)[5,6]fullerene

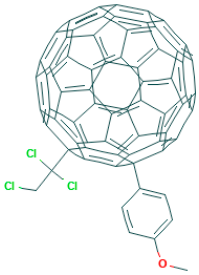

CID_101382121
$C_{62}F_6$
1,9-Bis(trifluoromethyl)(C_{60}-Ih)[5,6]fullerene

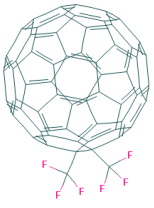

CID_10909337
$C_{66}HF_{12}I$
9-(1,1,2,2,3,3,4,4,5,5,6,6-Dodecafluoro-6-iodohexyl)-1H-(C_{60}-Ih)[5,6]fullerene

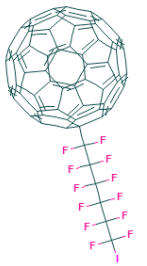

Figure 4. Graphic representation of functionalized fullerenes C_{60}.

For the transposition of cisPt at the cellular level through numerous barriers and to avoid their connection with the B group vitamins [7], an attempt was made to deposit Cisplatin on rhombellanes and functionalized fullerenes C_{60}, as possible nanodrug complexes. The symmetry of the analyzed nanostructures is an important factor determining the mutual affinity of the tested ligand and nanocarriers.

Detailed analysis of structural properties after docking showed many interesting features. Behavior of Cisplatin with respect to rhombellane homeomorphs and functionalized fullerenes C_{60}, in terms of their (interacting) energy, geometry and topology, was studied. After the docking procedure, the optimal values of ligand-rhombellane and ligand- C_{60} fullerene affinities were found, which is an important result for homeomorphs.

2. Methods

2.1. Docking Procedure

The structures of rhombellane homeomorphs were prepared by Topo Cluj Group [8–13], while the functionalized C_{60} structures were downloaded from the PubChem Database [22]. The docking procedure was realized with the use of non-commercial docking program AutoDock 4.2 [23,24]. This employs a stochastic Lamarckian genetic algorithm for computing ligand conformations and simultaneously minimizing its scoring function, which approximates the thermodynamic stability of the ligand bound to the target fullerene. For all considered nanocarriers there were established grid box dimensions equal to 26 × 26 × 26 Å. The center of the grid box was placed in the center of the considered nanomolecules. In most cases, the center of the grid box had xyz coordinates equal to 000. During the docking procedure, the molecules were loaded and stored as pdb-files, after assigning hydrogen bonds. The investigated ligands were loaded, and their torsions along the rotatable bonds were assigned and then saved as "ligand.pdbqt". The grid menu after loading "pdbqt" was toggled [25]. For the search of the ligand–Rbl nanostructure and ligand-C_{60} interactions, the map files were selected directly, setting up the grid points separately for each structure. The Lamarckian genetic algorithm completed the docking parameter files [26]. The structural analysis of the obtained complexes related with the identification of hydrogen bonds was realized with use of the Visual Molecular Dynamics (VMD) package [27].

2.2. Results and Discussion

The results are presented in the following tables and figures. Rhombellane structures are given by their atom number.

Table 1 and Figure 5 represent binding affinity in kcal/mol of the ligand cisPt molecule relative to spherical nanosystems, such as rhombellane structures (first eleven structures in tables) and functionalized fullerene C_{60} (structures 12 to 21 in tables) obtained during docking stage.

Table 1. Values of binding affinity [kcal/mol] of the ligand CisPt molecule relative to spherical nanosystems (rhombellane structures and functionalized fullerene C_{60}) obtained during the docking stage, generated by software Autodock 4.2.

	Binding Energy (kcal/mol)									
360b	−2.66	−2.6	−2.61	−2.49	−2.45	−2.42	−2.33	−2.44	−2.25	−2.42
372	−2.51	−2.38	−2.36	−2.31	−2.25	−2.25	−2.3	−2.2	−2.19	−2.17
396	−2.34	−2.29	−2.28	−2.19	−2.23	−2.23	−2.22	−2.22	−2.16	−2.13
420	−2.17	−2.16	−2.16	−2.16	−2.16	−2.16	−2.16	−2.09	−2.09	−2.09
444	−2.72	−2.71	−2.72	−2.69	−2.67	−2.67	−2.65	−2.63	−2.63	−2.63
456	−2.62	−2.62	−2.56	−2.56	−2.56	−2.55	−2.52	−2.45	−2.43	−2.41
ADA132	−2.3	−2.23	−2.27	−2.26	−2.23	−2.05	−2.16	−2.16	−2.04	−1.98
308a4	−2.16	−2.11	−1.97	−2.16	−2.14	−2.14	−2.14	−2.04	−1.95	−1.84
308b4	−2.09	−1.9	−2.08	−2.01	−1.98	−2.05	−1.94	−1.89	−1.84	−1.8
360a	−2.35	−2.23	−2.23	−2.17	−2.11	−2.22	−2.19	−2.17	−2.09	−2.02

Table 1. *Cont.*

	Binding Energy (kcal/mol)									
stf114	−1.9	−1.88	−1.87	−1.85	−1.78	−1.83	−1.76	−1.74	−1.82	−1.67
CID_11332103	−2.47	−2.47	−2.41	−2.41	−2.4	−2.4	−2.4	−2.37	−2.35	−2.19
CID_11468612	−2.54	−2.53	−2.51	−2.51	−2.5	−2.49	−2.48	−2.47	−2.47	−2.46
CID_16146387	−2.1	−2.09	−2.08	−2.08	−2.06	−2.01	−2	−2.06	−2.05	−2.04
CID_16150529	−2.14	−2.1	−2.09	−2.06	−2.04	−2.02	−1.98	−1.98	−1.97	−1.97
CID_16156307	−3.44	−3.41	−3.39	−3.37	−3.37	−3.37	−3.36	−3.36	−3.35	−3.33
CID_71619159	−1.74	−1.67	−1.73	−1.72	−1.57	−1.57	−1.56	−1.53	−1.49	−1.48
CID_101218232	−2.83	−2.82	−2.77	−2.76	−2.71	−2.63	−2.48	−2.46	−2.45	−2.4
CID_101218236	−3.13	−3.09	−3.07	−3.06	−3.05	−2.98	−2.93	−2.92	−2.91	−2.79
CID_101382121	−0.82	−0.8	−0.78	−0.78	−0.75	−0.8	−0.8	−0.77	−0.74	−0.73
CID_10909337_C	−0.97	−0.96	−0.96	−0.96	−0.96	−0.95	−0.94	−0.94	−0.94	−0.93

Among Rbl homeomorphs, Cisplatin has the highest affinity for Rbl 444 with an affinity value of −2.72 kcal/mol and for Rbl 360b with an affinity value of −2.66 kcal / mol (Table 1, Figure 5). The lowest binding energy is observed in the case of Staffanes (stf) 114 (Table 1, Figure 5). Among functionalized structures of C_{60} fullerene, the best affinity is shown by CID_16156307, followed by CID_10121832 and finally the CID_10121831 structure with values of affinity equal to −3.44, −3.13 and −2.83 kcal/mol, respectively (Table 1, Figure 5).

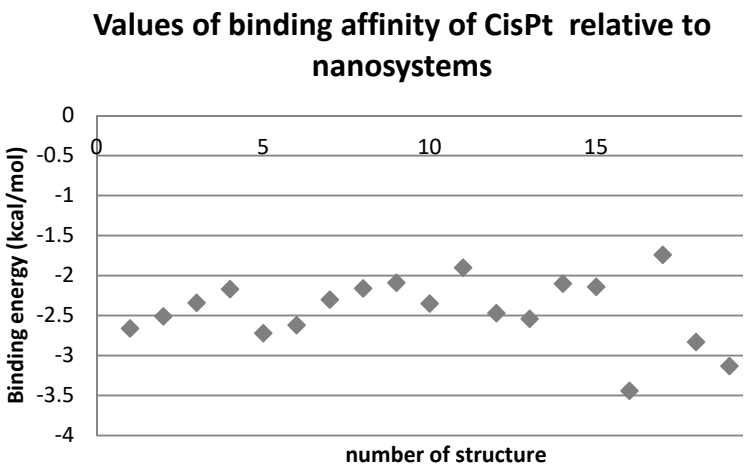

Structure	Nr	Binding energy
360b	1	−2.66
372	2	−2.51
396	3	−2.34
420	4	−2.17
444	5	−2.72
456	6	−2.62
ADA132	7	−2.3
308a4	8	−2.16
308b4	9	−2.09
360a	10	−2.35
stf114	11	−1.9
CID_11332103	12	−2.47
CID_11468612	13	−2.54
CID_16146387	14	−2.1
CID_16150529	15	−2.14
CID_16156307	16	−3.44
CID_71619159	17	−1.74
CID_101218232	18	−2.83
CID_101218236	19	−3.13
CID_101382121	20	−0.82
CID_10909337	21	−0.97

Figure 5. Graphical presentation of the values of binding affinity [kcal/mol] of the ligand CisPt molecule relative to spherical nanosystems (rhombellane structures and functionalized fullerene C_{60}) obtained during docking stage, generated by software Autodock 4.2.

In general, the examined structures show a significantly larger affinity in the case of C_{60} functionalized fullerene than in the case of Rbl homeomorphs. The obtained affinity values are collected in Tables 2 and 3.

Table 2. The best binding affinity of ligand CisPt, maximum and minimum bind energy, and Kmax values of the binding constant estimated with use of the binding free energy obtained for the best complex of ligand with nanostructure Rbl after the docking procedure, generated by software Autodock 4.2.

Name of Nanostructure	Maximum Binding Energy	Minimum Binding Energy	Average	SD	Binding Constant [K_{max}]
360b	−2.66	−2.25	−2.47	0.12	89.1
372	−2.51	−2.17	−2.29	0.10	69.2
396	−2.34	−2.13	−2.23	0.06	51.9
420	−2.17	−2.09	−2.14	0.03	39.0
444	−2.72	−2.63	−2.67	0.03	98.6
456	−2.62	−2.41	−2.53	0.07	83.3
ADA132	−2.30	−1.98	−2.17	0.10	48.5
308a4	−2.16	−1.84	−2.07	0.11	38.3
308b4	−2.09	−1.80	−1.96	0.10	34.0
360a	−2.35	−2.02	−2.18	0.09	52.8
stf114	−1.90	−1.67	−1.81	0.07	24.7

The values of binding energy are correlated with values of the K_{max} constant and the highest values are obtained in the case of 444 fullerene and 360b nanostructure (Table 2).

The two last columns show the equilibrium K value of the bonds, calculated using the equation:

$$K_B = exp^{(-\frac{\Delta G_b}{R\,T})}$$

where K_b is the binding constant, R is the gas constant (J/mol*K), T is the temperature of 298 K and ΔG_b is the binding affinity (J/mol).

The higher the K value, the more the reaction proceeds towards the formation of the complex.

Table 3. The best binding affinity of the ligand CisPt, maximum and minimum binding energy and Kmax values of the binding constant estimated with use of the binding free energy obtained for the best complex of the ligand with functionalized fullerene C_{60} after the docking procedure, generated by software Autodock 4.2.

Name of Nanostructure	Maximum Binding Energy	Minimum Binding Energy	Average	SD	Binding Constant [K_{max}]	Type
CID_11332103	−2.47	−2.19	−2.39	0.07	64.6	$C_{67}H_{14}F_3O_4P$
CID_11468612	−2.54	−2.46	−2.50	0.03	72.8	$C_{65}H_{13}O_3P$
CID_16146387	−2.10	−2.00	−2.06	0.03	34.6	$C_{67}H_{16}O_2Si$
CID_16150529	−2.14	−1.97	−2.04	0.06	37.0	$C_{70}H_{20}N_2O_2$
CID_16156307	−3.44	−3.33	−3.38	0.03	332.3	$C_{72}H_9F_2OP$
CID_71619159	−1.74	−1.48	−1.61	0.09	18.9	$C_{68}H_{10}O_2$
CID_101218232	−2.83	−2.40	−2.63	0.16	118.7	$C_{63}H_4ClF_3O$
CID_101218236	−3.13	−2.79	−2.99	0.10	196.9	$C_{69}H_9Cl_3O$
CID_101382121	−0.82	−0.73	−0.78	0.03	4.0	$C_{62}F_6$
CID_10909337	−0.97	−0.93	−0.95	0.01	5.1	$C_{66}HF_{12}I$

Table 3 presents K_{max} values of the binding constant estimated with use of the binding free energy obtained for the best complex of the ligand with functionalized fullerene C_{60}. The highest values of the binding energy are also here correlated with values of the constant K_{max}. This value is higher in the case of derivatives CID_16156307 of C_{60} fullerene, followed by CID_101218236 and CID_101218232 (Table 3).

Cisplatin (cisPt) and functionalized fullerene C_{60} easily create two or three hydrogen bonds between them with strong and medium strength (Figure 6).

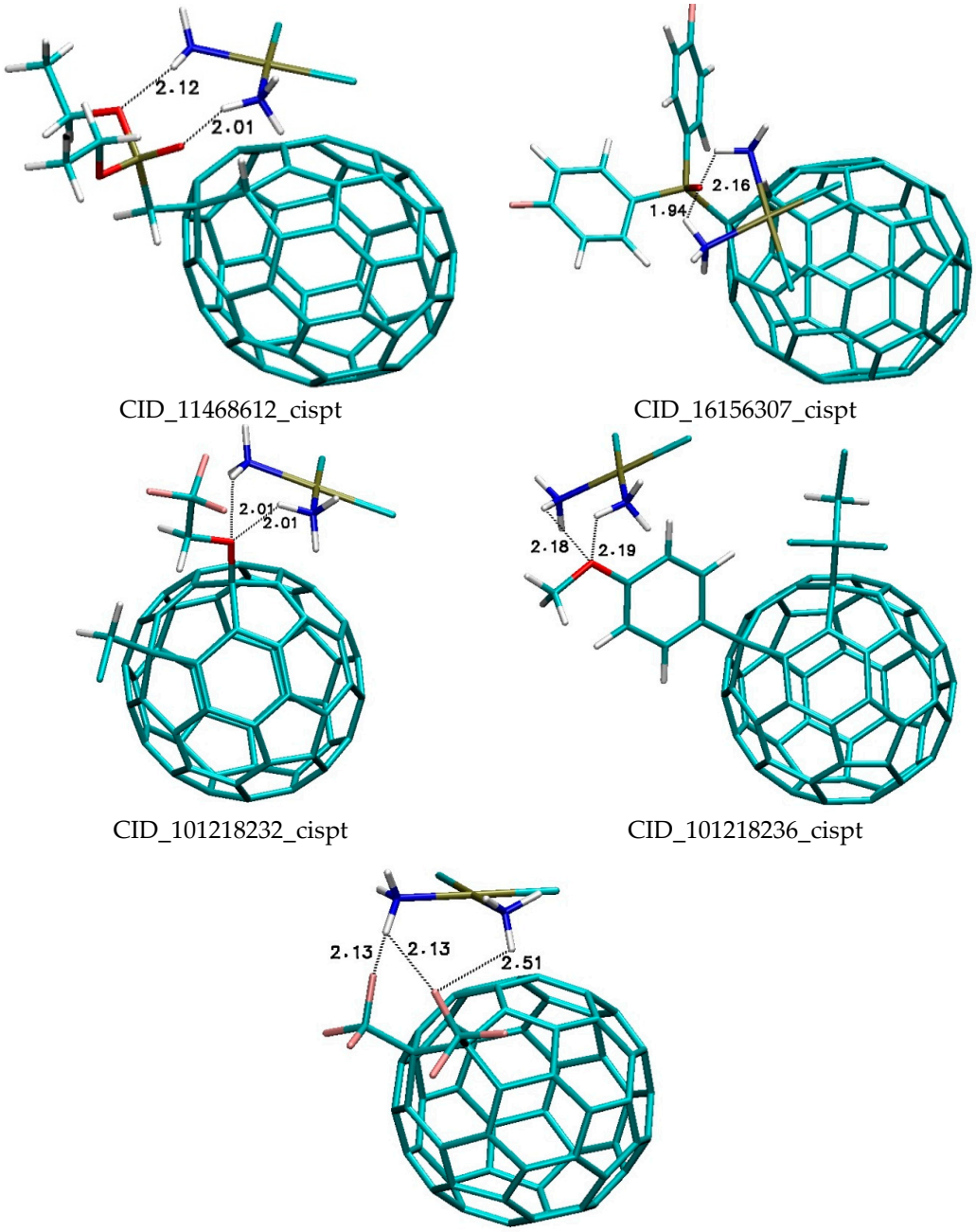

Figure 6. The structure of functionalized fullerene C_{60} and Cisplatin complexes.

The criterion for classification of the strength of hydrogen bonds is the assessment of the distance between acceptor and hydrogen atoms: strong interactions are characterized by a distance <1.6 Å, medium by values in the range from 1.6 Å to 2.0 Å, and weak by distances <3 Å.

The complex nanostructure CID_16156307 ($C_{72}H_9F_2OP$)–CisPt has been created by two hydrogen bonds with medium strengths, i.e., 1.94 Å and 2.16 Å; both are between the oxygen of the phosphoryl group of the nanocarrier and the hydrogen of the amino groups of cisPt (Figure 6). Again, two hydrogen bonds have been created in the case of CID_ 101218236 ($C_{69}H_9Cl_3O$) and CID_101218232 ($C_{63}H_4ClF_3O$) complexes. The first case involves the oxygen atom of the methoxy group while the second involves the oxygen atom of the ethoxy group, and both form a Hydrogen Bond (HB) with the hydrogen atom of the amino groups of cisPt with values 2.18 Å, 2.19 Å and 2.01 Å (Figure 6). Three hydrogen bonds appeared

only in the case of CID_10138212 ($C_{62}F_6$), all with medium strength, i.e., 2.13 Å, 2,13 Å and 2.51 Å (Figure 6), respectively. The structures of formed complexes are presented in Figure 6.

Despite the fact that affinity is higher in the case of functionalized fullerene C_{60}–cisPt, compared to affinities of Rbl–CisPt complexes, the latter created a larger number of hydrogen bonds (Figure 7). The best binding energy has been observed for the 444 nanostructure with four hydrogen bonds of medium strength, i.e., 1.88 Å, 1.95 Å, 1.96 Å and 2.03 Å, respectively. Also, for the 360b nanostructure there were created four hydrogen bonds with medium strength, i.e., 2.08 Å, 2.09 Å, 2.26 Å and 2.56 Å, respectively (Figure 7). The worst affinity is represented by the stf114 fullerene. Even so, in this case there are also four hydrogen bonds formed between the nanostructure and Cisplatin. The structures of formed complexes are presented in Figure 7.

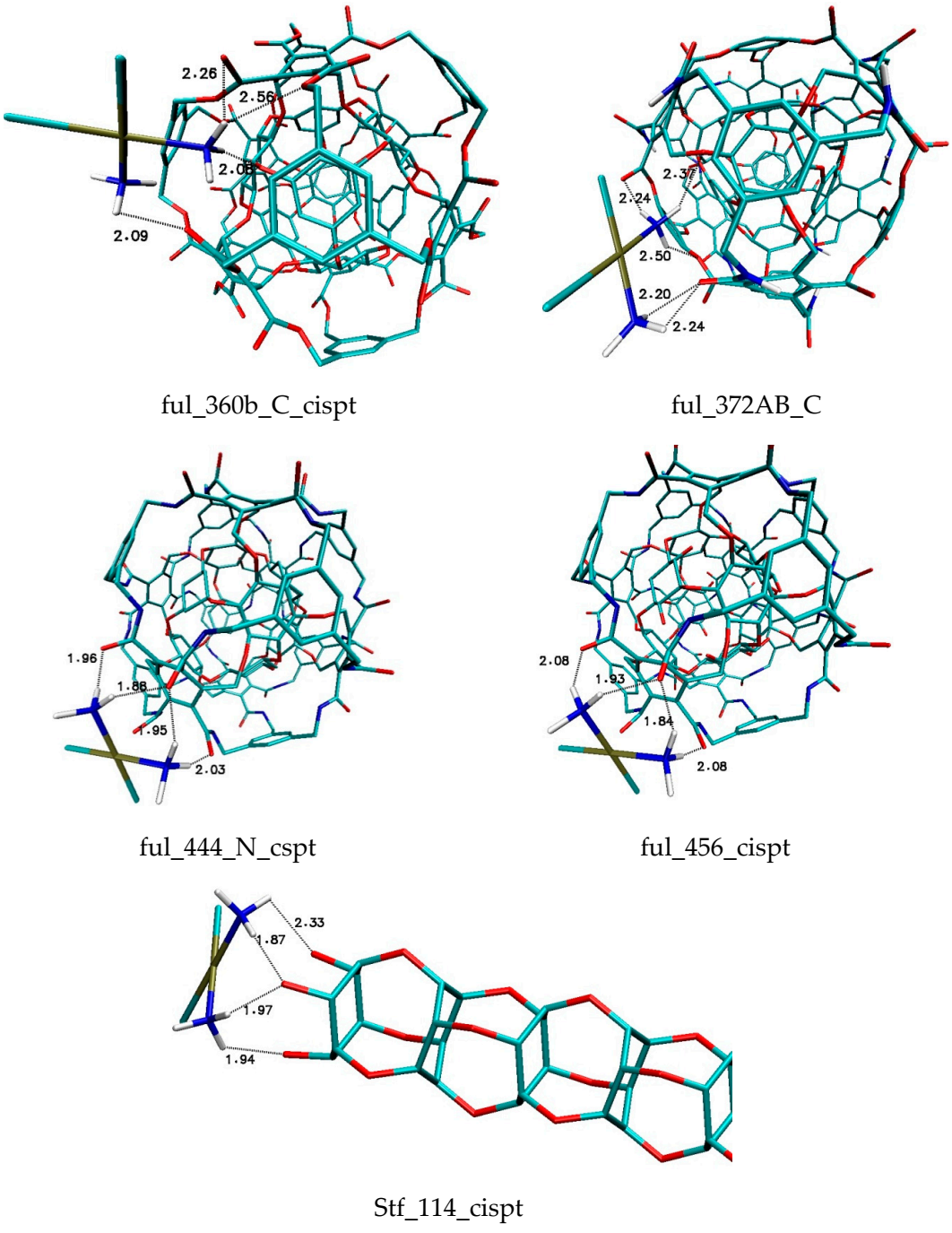

Figure 7. The structure of cube rhombellane and Cisplatin complexes.

3. Conclusions

As a proposal for a new nanodrug, an attempt was made to implement the Cisplatin (cisPt) ligand on the functionalized C_{60} fullerenes and on a cube rhombellane homeomorphic surface. Cisplatin (cisPt) is one of the strongest anticancer agents with proven clinical activity against a wide range of solid tumors. Theoretical studies suggest that nonspecific interactions of Cisplatin can also take place with many competitive compounds, such as vitamins of the B group, containing aromatic rings with lone-pair orbitals. It is argued that such a direct analogy to the interaction of canonical purines can impair the therapeutic effect of Cisplatin, which might be an indicator of the reduction of the anticancer therapeutic effects of the Cisplatin drug in the presence of vitamins of the B group inside the cell nucleus. This is why it seems to be important to connect cisPt Should be "cisPt" with nanostructures and, in this way, make it impossible to combine the drug with the B vitamins. Behavior of Cisplatin with respect to rhombellane homeomorphs and functionalized fullerenes C_{60}, in terms of their (interacting) energy, geometry and topology was studied. The symmetry of the analyzed nanostructures is an important factor determining the mutual affinity of the tested ligand and nanocarriers. The docking procedure was realized with use of AutoDock 4.2. Detailed analysis of structural properties after docking showed many interesting features. Among Rbl homeomorphs, Cisplatin has the highest affinity for Rbl 444 with an affinity value of −2.72 kcal/mol and Rbl 360b with an affinity value of −2.66 kcal/mol. Among functionalized structures of C_{60} fullerene the best affinity is shown by CID_16156307, followed by CID_10121832 and finally CID_10121831, with values of affinity equal to −3.44, −3.13 and −2.83 kcal/mol, respectively. In general, the examined structures show a significantly larger affinity in the case of C_{60} functionalized fullerene than in the case of Rbl homeomorphs. Cisplatin (cisPt) and functionalized fullerene C_{60} easily create two or three hydrogen bonds between them with strong and medium strength. High ligand-nanostructure affinity is reflected by the number and most of all the quality of formed hydrogen bonds. However, despite the fact that affinity is better in the case of functionalized fullerene C_{60}–cisPt compared with affinities of complexes Rbl–CisPt Should be "cisPt", the latter created a larger number of hydrogen bonds but of lesser quality. The performed investigations enabled the identification of the most promising rhombellane and functionalized C_{60} fullerene structures that could be used as nanocarriers for cisPt molecules.

Author Contributions: Conceptualization, B.S.; Methodology, B.S. and P.C.; Validation, B.S. and P.C.; Formal Analysis, B.S.; Investigation, B.S.; Resources, B.S.; Data Curation, B.S.; Writing–Original Draft Preparation, B.S.; Writing–Review & Editing, B.S. and P.C.; Visualization, B.S. and P.C.; Supervision, B.S.; Project Administration, B.S.; Funding Acquisition, B.S.

Acknowledgments: Gratitude is expressed for fruitful cooperation for many years to Professor MV Diudea; this article was supported by PL-Grid Infrastructure (http://www.plgrid.pl/en).

Conflicts of Interest: The authors declare no conflict of interest.

References

1. Frezza, M.; Hindo, S.; Chen, D.; Davenport, A.; Schmitt, S.; Tomco, D.; Dou, Q.P. Novel metals and metal complexes as platforms for cancer therapy. *Curr. Pharm. Des.* **2010**, *16*, 1813–1825. [CrossRef] [PubMed]
2. Desoize, B.; Madoulet, C. Particular aspects of platinum compounds used at present in cancer treatment. *Crit. Rev. Oncol. Hematol.* **2002**, *42*, 317–325. [CrossRef]
3. Fraval, H.N.; Rawlings, C.J.; Roberts, J.J. Increased sensitivity of UV-repair-deficient human cells to DNA bound platinum products which unlike thymine dimers are not recognized by an endonuclease extracted from micrococcus luteus. *Mutat. Res.* **1978**, *51*, 121–132. [CrossRef]
4. Wiernik, P.H.; Yeap, B.; Vogl, S.E.; Kaplan, B.H.; Comis, R.L.; Falkson, G.; Davis, T.E.; Fazzini, E.; Cheuvart, B.; Horton, J. Hexamethylmelamine and low or moderate dose cisplatin with or without pyridoxine for treatment of advanced ovarian carcinoma: A study of the eastern cooperative oncology group. *Cancer Invest.* **1992**, *10*, 1–9. [CrossRef] [PubMed]
5. Wiltshaw, E.; Kroner, T. Phase II study of cis-dichlorodiammineplatinum[II] (NSC-119875] in advanced adenocarcinoma of the ovary. *Cancer Treat. Rep.* **1976**, *60*, 55–60. [PubMed]

6. Dasari, S.; Tchounwou, P.B. Cisplatin in cancer therapy: Molecular mechanisms of action. *Eur. J. Pharmacol.* **2014**, *740*, 364–378. [CrossRef] [PubMed]
7. Szefler, B.; Czeleń, P.; Szczepanik, A.; Cysewski, P. Does affinity of cisplatin to B-Vitamins impair the therapeutic effect in the case of patient with lung cancer consuming carrot or beet juice? *Anticancer Agents Med Chem.* **2019**, *25*. [CrossRef] [PubMed]
8. ISI Web of Science. 2010.
9. Gomes, J.A.N.F.; Mallion, R.B. Aromaticity and ring currents. *Chem. Rev.* **2001**, *101*, 1349–1383. [CrossRef]
10. Cyrański, M.K.; Krygowski, T.M.; Katritzky, A.R.; Schleyer, P.v.R. To what extent can aromaticity be defined uniquely? *J. Org. Chem.* **2002**, *67*, 1333–1338. [CrossRef]
11. Chen, Z.; Wannere, C.S.; Crominboeuf, C.; Puchta, R.; Schleyer, R.v.P. nucleus-independent chemical shifts (NICS) as an aromaticity criterion. *Chem. Rev.* **2005**, *105*, 3842–3888. [CrossRef]
12. Diudea, M.V.; Lungu, C.N.; Nagy, C.L. Cube-rhombellane related structures: A drug perspective. *Molecules* **2018**, *23*, 2533. [CrossRef] [PubMed]
13. Diudea, M.V.; Pîrvan-Moldovan, A.; Pop, R.; Medeleanu, M. Medeleanu, Energy of graphs and remote graphs, in hypercubes, rhombellanes and fullerenes. *MATCH Commun. Math. Comput. Chem.* **2018**, *80*, 835–852.
14. Pauling, L.; Wheland, G.W. The nature of the chemical bond. V. The quantum mechanical calculation of the resonance energy of benzene and naphthalene and the hydrocarbon free radicals. *J. Chem. Phys.* **1933**, *1*, 362–374. [CrossRef]
15. Daudel, R.; Lefebre, R.; Moser, C. *Quantum Chemistry*; Interscience: New York, NY, USA, 1959.
16. Diudea, M.V. Rhombellanic diamond. Fullerenes, Nanotubes and Carbon. *Nanomaterials* **2018**. [CrossRef]
17. Pop, R.; Medeleanu, M.; Diudea, M.V.; Szefler, B.; Cioslowski, J. Fullerenes patched by flowers. *Cent. Eur. J. Chem.* **2013**, *11*, 527–534. [CrossRef]
18. Frisch, M.J.; Trucks, G.W.; Schlegel, H.B.; Scuseria, G.E.; Robb, M.A.; Cheeseman, J.R.; Scalmani, G.; Barone, V.; Mennucci, B.; Petersson, G.A.; et al. *Gaussian 09, Revision A.1*; Gaussian Inc.: Wallingford, CT, USA, 2009.
19. Randić, M. Aromaticity of Polycyclic Conjugated Hydrocarbons. *Chem. Rev.* **2003**, *103*, 3449–3605.
20. Diudea, M.V.; Nagy, C.L. *Periodic Nanostructures*; Springer: Dordrecht, The Netherlands, 2007.
21. Szefler, B. Nanotechnology, from quantum mechanical calculations up to drug delivery. *Int. J. Nanomed.* **2018**, *13*, 6143–6176. [CrossRef] [PubMed]
22. Pubchem. Available online: https://pubchem.ncbi.nlm.nih.gov// (accessed on 11 June 2019).
23. Morris, G.M.; Huey, R.; Lindstrom, W.; Sanner, M.F.; Belew, R.K.; Goodsell, D.S.; Olson, A.J. Autodock4 and AutoDockTools4: Automated docking with selective receptor flexibility. *J. Comput. Chem.* **2009**, *30*, 2785–2791. [CrossRef] [PubMed]
24. Shoichet, B.K.; Kuntz, I.D.; Bodian, D.L. Molecular docking using shape descriptors. *J. Comput. Chem.* **2004**, *13*, 380–397. [CrossRef]
25. Dhananjayan, K.; Kalathil, K.; Sumathy, A.; Sivanandy, P. A computational study on binding affinity of bio-flavonoids on the crystal structure of 3-hydroxy-3-methyl-glutaryl-CoA reductase—An insilico molecular docking approach. *Der Pharma Chemica.* **2014**, *6*, 378–387.
26. Abagyan, R.; Totrov, M. High-throughput docking for lead generation. *Current Opin. Chem. Biol.* **2001**, *5*, 375. [CrossRef]
27. Humphrey, W.; Dalke, A.; Schulten, K. VMD: Visual molecular dynamics. *J. Mol. Graph.* **1996**, *14*, 33–38. [CrossRef]